Mechanical Engineering Research; Vol. 6, No. 1; 2016
ISSN 1927-0607 E-ISSN 1927-0615
Published by Canadian Center of Science and Education

Dynamic Simulation of Adaptive Truss Consisting of Various Types of Truss Members

Kazuyuki Hanahara[1], Xuan Zhang[1] & Yukio Tada[1]

[1] Graduate School of System Informatics, Kobe University, Kobe, Japan

Correspondence: Kazuyuki Hanahara, Graduate School of System Informatics, Kobe University, Kobe, Japan. Tel: 81-78-803-6249. E-mail: hanahara@cs.kobe-u.ac.jp

Received: April 19, 2016 Accepted: April 26, 2016 Online Published: April 28, 2016

doi:10.5539/mer.v6n1p75 URL: http://dx.doi.org/10.5539/mer.v6n1p75

Abstract

An adaptive truss is a truss structural system equipped with functional truss members, such as length-adjustable members, shape memory alloy (SMA) members, spring-dashpot members, and so on. This is a representative example of so-called adaptive structure. In this study, we deal with the dynamic simulation of various types of adaptive trusses. The geometrical relation is given in a universal form applicable to all planar and spatial trusses. We develop descriptions of dynamic behavior of various types of functional truss members and give a general form of the descriptions. The equation of motion is formulated based on the geometrical relation and the description of member characteristics. Dynamics simulation procedure based on the Newmark β method is also developed. Dynamic behaviors of several types of adaptive trusses are simulated. The feasibility of the proposed dynamics calculation is confirmed; some characteristic dynamic behaviors of adaptive trusses are demonstrated.

Keywords: adaptive truss, variable geometry truss, dynamics, simulation, wire, spring-dashpot, shape memory alloy

1. Introduction

An adaptive truss is a truss structural system equipped with a number of functional truss members, such as length-adjustable members, shape memory alloy (SMA) members, spring-dashpot members, and so on. It is a typical example of so-called adaptive structure, which is a structural system that has the ability to exhibit geometrical or mechanical adaptability (Wada et al., 1990).

One of such examples is a variable geometry truss (VGT) consisting of a number of length-adjustable actuated members (Miura et al., 1985). Adjusting its actuated truss member lengths, it can change its geometry as well as its mechanical characteristics. This type of mechanical system is expected to be a useful instrument for space missions, such as a space crane (Ramesh et al., 1990), a robotic manipulator (Hughes et al., 1991), a docking mechanism (Senda et al., 1995), a momentum management mechanism (Hanahara & Tada, 2002), and other promising applications.

A conventional type of VGT or adaptive truss is consisting of length-adjustable members accommodated with a telescopic type actuator and their truss topology is statically determinate (Tanaka et al., 1991). Other types of adaptive trusses are, however, also possible. A truss having length-adjustable wire members is one example (Hanahara & Tada, 2000; Hanahara & Tada, 2004; Hanahara et al., 2006). Owing to the lack of compressive rigidity of a wire truss member, this type of truss has to have a statically indeterminate topology; however, wire member actuators are expected to be of large stroke and light-weight.

An adaptive truss having SMA wire members is also possible (Hanahara & Tada, 2008; Hanahara & Tada, 2014). Dos Santos et al. (2015) refers to this type of mechanical system as an adaptive shape-morphing tensegrity structure. SMA wire has the striking capability to change its length by itself by Joule heating (Lagoudas, 2008); that is, actuation mechanisms are not necessary for this type of adaptive truss.

In the current study, we deal with dynamic simulation of these various types of adaptive trusses. Seguchi et al. (1990) have reported dynamic simulation of truss-type robot arm consisting of ordinary rigid length-adjustable truss members. In order to deal with wire truss members, however, we have to take into account the conspicuous characteristics of wire that it does not have any compressive stiffness. In order to deal with SMA truss members,

we have to take into account its nonlinear and hysteretic characteristics. We formulate the equation of motion in general form, that takes into account all of these situations. In addition to ordinary rigid length-adjustable members, spring-dashpot members, wire members, and SMA members are dealt with in this study. Dynamic calculation procedure based on the Newmark β method (Newmark, 1959) is also proposed.

A number of example dynamic simulations of various types of adaptive trusses are conducted. The feasibility of the proposed dynamics calculation is confirmed; influence of the mechanical characteristics of truss members on the dynamic behavior of the adaptive truss system are also demonstrated.

2. Truss Structure System Dealt with in This Study

We give a brief introduction of adaptive trusses. The geometrical relation between the member lengths and the nodal positions in general form is also introduced.

2.1 Variable Geometry Truss, Adaptive Truss, Smart Truss

Truss is a simple structural system conceptually consisting only of truss members and truss nodes. Implementing functional truss members, it can exhibit various types of mechanical and geometrical characteristics. A typical example is the VGT, the variable geometry truss (Miura et al., 1985), that has the ability to change its geometry by means of the length-adjustable truss members. This type of mechanical system is also referred to as an adaptive truss (Chen & Wada, 1993). Tanaka et al. (1991) give its kinematical relation taking into account the practical considerations of nodal offset. Yang et al. (2005) report a smart truss that adopts truss members equipped with piezoelectric elements, aiming to suppress the structural vibration. The authors have reported adaptive trusses consisting of length-adjustable wire members (Hanahara & Tada, 2004; Hanahara et al., 2006) and SMA wire members (Hanahara & Tada, 2008; Hanahara & Tada, 2014). In contrast to the conventional VGT, these adaptive trusses with wire members must have a statically indeterminate topology.

2.2 Kinematics — Geometrical Relation

We deal with adaptive truss structures having the ability to change its geometry as well as its mechanical characteristics. This type of mechanical system is considered to be a kind of parallel robot (Merlet, 2006) or a variant of so-called platform (Stewart, 1965-66; Dunlop & Garcia, 2002) as well. The kinematical relation is formulated based on the geometrical relation.

For a truss structural system, the basic geometrical relation is expressed in terms of the distance between two nodes corresponding to the length of the member connecting them. In the case that the ith member connects the two nodes, $\alpha(i)$ and $\beta(i)$, its length l_i is corresponding to the distance between the two nodal positions $\boldsymbol{x}_{\alpha(i)}$ and $\boldsymbol{x}_{\beta(i)}$. This geometrical relation is expressed as

$$l_i = \left[(\boldsymbol{x}_{\alpha(i)} - \boldsymbol{x}_{\beta(i)})^T (\boldsymbol{x}_{\alpha(i)} - \boldsymbol{x}_{\beta(i)}) \right]^{(1/2)} \tag{1}$$

On the basis of Equation (1), we obtain the following expression in vector form:

$$\boldsymbol{l} = \boldsymbol{f}(\boldsymbol{X}) \tag{2}$$

where $\boldsymbol{l} = [l_1, \cdots, l_M]^T$ is the total member lengths vector and $\boldsymbol{X} = [\boldsymbol{x}_1^T, \cdots, \boldsymbol{x}_N^T]^T$ is the total nodal positions vector. The total differential of Equation (2) is expressed as

$$d\boldsymbol{l} = \frac{\partial \boldsymbol{l}}{\partial \boldsymbol{X}} d\boldsymbol{X} \tag{3}$$

The Jacobian matrix is given as

$$\frac{\partial \boldsymbol{l}}{\partial \boldsymbol{X}} = \left[\frac{\partial l_i}{\partial \boldsymbol{x}_n} \right] \quad (i = 1, \cdots, M,\ n = 1, \cdots, N) \tag{4}$$

where

$$\frac{\partial l_i}{\partial \boldsymbol{x}_n} = \begin{cases} \dfrac{1}{l_i} (\boldsymbol{x}_{\alpha(i)} - \boldsymbol{x}_{\beta(i)})^T & (n = \alpha(i)) \\ \dfrac{1}{l_i} (\boldsymbol{x}_{\beta(i)} - \boldsymbol{x}_{\alpha(i)})^T & (n = \beta(i)) \\ 0 & (\text{other}) \end{cases} \tag{5}$$

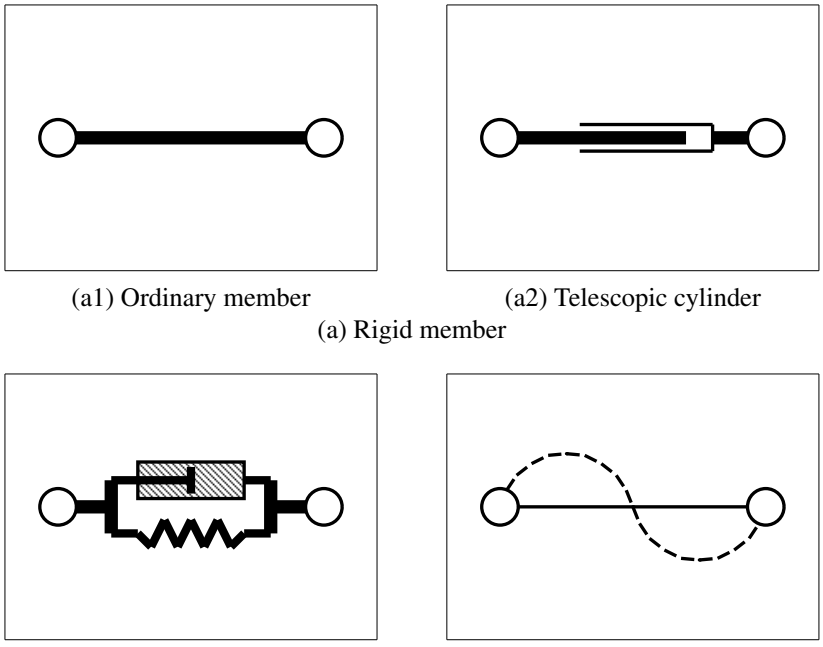

(a1) Ordinary member (a2) Telescopic cylinder

(a) Rigid member

(b) Spring-dashpot member (c) Wire member

Figure 1. Conceptual illustration of various types of truss members

These geometrical relations are crucial to deal with the kinematics and dynamics of VGTs or adaptive trusses. In the case of dealing with the inverse kinematics, Equation (3) is solved for $d\boldsymbol{l}$ under some adequate conditions. It should be noted that the above formulation is independent of the dimension of space.

3. Models of Truss Member Behavior

Mechanical behaviors of truss members of various types are taken into consideration. A formulation in general form is also developed.

3.1 Rigid Member

This is a simple ordinary truss member as shown in Figure 1(a1). It can also be of length-adjustable telescopic cylinder as shown in Figure 1(a2), in the case of the statically determinate VGT. The mechanical behavior of *i*th truss member of this type can be expressed as

$$p_i = k_i(r_i + l_i - \rho_i) = k_i r_i + k_i(l_i - \rho_i) = k_i r_i + q_i \tag{6}$$

where p_i is the axial force, r_i is the relative elastic deformation, l_i is the reference length, ρ_i is the neutral length corresponding to zero axial force, and k_i is the axial stiffness. The offset axial force q_i, where $q_i = k_i(l_i - \rho_i)$ in the above equation, is introduced for generality and for the compatibility with the following formulations of other types of truss members. A conventional model of the stiffness is given as

$$k_i = E_i A_i / \rho_i \tag{7}$$

where E_i is the Young's modulus and A_i is the cross-sectional area. In the case of an ordinary non-actuated truss member, Equation (6) is reduced to

$$p_i = k_i r_i \tag{8}$$

by putting $l_i = \rho_i$.

3.2 Spring-Dashpot Member

Truss members of this type can be applicable in order to improve the oscillation damping capability. A conceptual illustration of spring-dashpot member is shown in Figure 1(b). The mechanical behavior in this case is expressed as

$$p_i = k_i r_i + c_i \dot{h}_i + q_i \tag{9}$$

where c_i is the damping coefficient, $h_i = l_i + r_i$ is the total length and q_i is the offset axial force corresponding to the current reference length l_i. In the typical case that the spring is linearly elastic and the adopted l_i is fixed to its corresponding neutral position, Equation (9) is reduced to

$$p_i = k_i r_i + c_i \dot{r}_i \tag{10}$$

In the case of taking account of nonlinearity of the spring and the dashpot, the parameters in Equation (9), k_i, c_i, and q_i, become functions of the reference length l_i, which should be accordingly updated.

3.3 Wire/Cable Member

In the case of truss structure system of statically indeterminate topology, wire or cable truss members can be applicable. Truss members of this type are light-weight and to be expected to have large stroke by means of winding and unwinding from the viewpoint of length-adjustability; they cannot take, however, any compressive force. A conceptual illustration is given in Figure 1(c).

The mechanical behavior is expressed similarly to Equation (6); however, since a wire does not have any compressive stiffness, the mechanical behavior in this case is expressed as

$$p_i = \begin{cases} k_i r_i + q_i & (r_i + l_i \geq \rho_i) \\ 0 \ (k_i = q_i = 0) & (r_i + l_i < \rho_i) \end{cases} \tag{11}$$

The equation can also be reduced to

$$p_i = \begin{cases} k_i r_i & (r_i \geq 0) \\ 0 \ (k_i = 0) & (r_i < 0) \end{cases} \tag{12}$$

in the case of $l_i = \rho_i$.

3.4 SMA Member

Adopting shape memory alloy (SMA) truss members, a truss structure is expected to have the ability of geometry adaptation by means of the shape memory effect, as well as the capability of vibration energy dissipation by means of the hysteretic mechanical characteristic. An illustrative mechanical behavior and its typical piecewise linear model of SMA are shown in Figure 2. As shown in these figures, the stress-strain relation of SMA is highly nonlinear and the material stiffness significantly depends on the direction of deformation progression especially in a case such as the piecewise linear model shown in Figure 2(b). Taking the characteristics into consideration, we express the Young's modulus of SMA member i in the following form as:

$$E_i = E_i(\epsilon_i, \sigma_i, \mathrm{sgn}(\dot{\epsilon}_i), T_i) \tag{13}$$

where σ_i and ϵ_i are the stress and strain and $\mathrm{sgn}(\dot{\epsilon}_i)$ is adopted to take account of the deformation progressing direction. Material temperature T_i determines the overall characteristics of the SMA truss member. Strain ϵ_i and

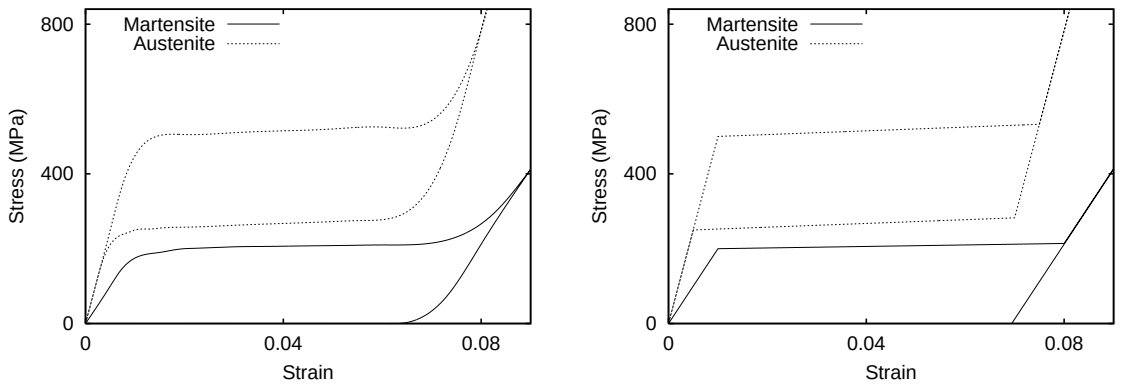

(a) Typical behavior (b) Piecewise linear model

Figure 2. Mechanical characteristic of shape memory alloy

stress σ_i denote the current material state of the ith member under the temperature condition of T_i in this model. On the basis of the corresponding reference length l_i, strain ϵ_i is expressed as

$$\epsilon_i = (l_i - \underline{l}_i)/\underline{l}_i \tag{14}$$

where $\underline{l}_i$ denotes the natural length of SMA member corresponding to zero strain. The mechanical behavior of SMA truss member is then expressed as

$$p_i = k_i r_i + q_i \tag{15}$$

where $k_i = E_i A_i / l_i$ and $q_i = \sigma_i A_i$. In the calculation process of the behavior of SMA truss member, reference length l_i as well as the corresponding strain ϵ_i, and stress σ_i are updated in accordance with the changing material state; Young's modulus E_i, member stiffness k_i and axial force offset q_i are updated accordingly as well.

In the case that SMA member i is a wire, Equation (15) is rewritten in the same form as Equation (11) as

$$p_i = \begin{cases} k_i r_i + q_i & (r_i + l_i \geq \rho_i) \\ 0 \ (k_i = q_i = 0) & (r_i + l_i < \rho_i) \end{cases} \tag{16}$$

where ρ_i denotes the current neutral length corresponding to zero axial force without slack. It should be noted that this ρ_i is not constant in general even in the case of constant $\underline{l}_i$, since there can be a residual deformation under zero axial force in the case that the SMA member is in the martensitic phase.

3.5 Model in General Form

On the basis of the above consideration, we adopt the following model of mechanical behavior of truss members in general form:

$$p_i = k_i r_i + c_i \dot{h}_i + q_i \tag{17}$$

where k_i, c_i and q_i are not always constant and expressed as the function of reference length l_i and other various state quantities $\mathcal{S}_i$ of truss member i, that is

$$k_i = k_i(l_i, \mathcal{S}_i), \qquad c_i = c_i(l_i, \mathcal{S}_i), \qquad q_i = q_i(l_i, \mathcal{S}_i) \tag{18}$$

The parameters included in $\mathcal{S}_i$ depend on the type of truss member i as well as the details of the adopted mechanical model. The condition expressed as Equation (11) or Equation(16) should also be taken into consideration in the case of a wire member.

4. Equation of Motion

We denote the position of the nth node of the truss system taking into account the deformation as $\boldsymbol{d}_n$, where $\boldsymbol{d}_n$ is a 2D or 3D vector corresponding to planer or spatial truss structure. The total nodal positions vector taking account of the deformation is expressed as $\boldsymbol{D} = [\boldsymbol{d}_1^T, \cdots, \boldsymbol{d}_N^T]^T$, where N is the number of truss nodes. The total vectors corresponding to member lengths are expressed as $\boldsymbol{l} = [l_1, \cdots, l_M]^T$, $\boldsymbol{r} = [r_1, \cdots, r_M]^T$, $\boldsymbol{h} = [h_1, \cdots, h_M]^T$, and so on; the total member axial force vector is similarly expressed as $\boldsymbol{p} = [p_1, \cdots, p_M]^T$. On the basis of the Jacobian matrix between the geometrical member lengths and the nodal positions $\boldsymbol{J} = \partial \boldsymbol{h} / \partial \boldsymbol{D}$, which can be obtained as in 2.2, the equation of motion of truss structure system is expressed as

$$\boldsymbol{M}\ddot{\boldsymbol{D}} = \boldsymbol{F} - \boldsymbol{J}^T \boldsymbol{p} \tag{19}$$

where $\boldsymbol{M}$ is the nodal inertia matrix and $\boldsymbol{F}$ is the external nodal force vector. The term of nodal force due to the member force, $\boldsymbol{J}^T \boldsymbol{p}$, is based on the standard approach dealt with in the field of robotics (Craig, 1989) and the minus sign represents that the tensile member force p_i is positive in the contracting direction.

Substituting Equation (17) into Equation (19) in terms of matrices and vectors, we obtain

$$\boldsymbol{M}\ddot{\boldsymbol{D}} = \boldsymbol{F} - \boldsymbol{J}^T(\boldsymbol{K}_r \boldsymbol{r} + \boldsymbol{C}_h \dot{\boldsymbol{h}} + \boldsymbol{q}) \tag{20}$$

where $\boldsymbol{K}_r = \mathrm{diag}[k_1, \cdots, k_M]$, $\boldsymbol{C}_h = \mathrm{diag}[c_1, \cdots, c_M]$, and $\boldsymbol{q} = [q_1, \cdots, q_M]^T$. Since the member lengths velocity is linearly related to the nodal velocity as $\dot{\boldsymbol{h}} = \boldsymbol{J}\dot{\boldsymbol{D}}$, Equation (20) is rewritten as follows:

$$\boldsymbol{M}\ddot{\boldsymbol{D}} + \boldsymbol{C}\dot{\boldsymbol{D}} + \boldsymbol{J}^T \boldsymbol{K}_r(\boldsymbol{f}(\boldsymbol{D}) - \boldsymbol{l}) = \boldsymbol{F} - \boldsymbol{J}^T \boldsymbol{q} \tag{21}$$

where

$$\boldsymbol{C} = \boldsymbol{J}^T \boldsymbol{C}_h \boldsymbol{J} \tag{22}$$

is the nodal damping matrix and the relative elastic deformation is expressed in terms of the nodal positions, referring to the geometrical relation (2), as

$$\boldsymbol{r} = \boldsymbol{f}(\boldsymbol{D}) - \boldsymbol{l} \tag{23}$$

Equation (21) is the equation of motion of adaptive truss structure system in general form dealt with in the current study.

Consider the case that the truss structure system consists only of ordinary non-actuated members as well as spring-dashpot members of small stroke. We take the reference lengths to the neutral; that is $\boldsymbol{l} = \boldsymbol{\rho} = \boldsymbol{f}(\boldsymbol{X})$, where $\boldsymbol{X}$ is the initial constant neutral non-deformed nodal positions. This leads to $\boldsymbol{q} = 0$. The nodal displacements vector is expressed as $\boldsymbol{U} = \boldsymbol{D} - \boldsymbol{X}$ and the member deformation can be linearly related as $\boldsymbol{r} = \boldsymbol{f}(\boldsymbol{D}) - \boldsymbol{l} = \boldsymbol{J}\boldsymbol{U}$ in this case. The equation of motion (21) is then reduced to the following conventional form as

$$\boldsymbol{M}\ddot{\boldsymbol{U}} + \boldsymbol{C}\dot{\boldsymbol{U}} + \boldsymbol{K}\boldsymbol{U} = \boldsymbol{F} \tag{24}$$

where

$$\boldsymbol{K} = \boldsymbol{J}^T \boldsymbol{K}_r \boldsymbol{J} \tag{25}$$

is the nodal stiffness matrix. In this case, the matrices $\boldsymbol{M}$, $\boldsymbol{C}$, and $\boldsymbol{K}$ are assumed to be constant.

5. Dynamic Calculation

The dynamic simulation based on the equation of motion formulated in the previous section is performed by means of a numerical integration. Calculation of Equation (21) based on the Newmark β method (Newmark, 1959) is formulated and a numerical simulation procedure taking into account the conditions of various truss members is developed.

5.1 Discretization by Means of Newmark β Method

The nodal positions vector is discretized by means of the Newmark β method as

$$\boldsymbol{D}^{(n+1)} = \boldsymbol{D}^{(n)} + \Delta t \dot{\boldsymbol{D}}^{(n)} + \frac{\Delta t^2}{2}\left\{(1-2\beta)\ddot{\boldsymbol{D}}^{(n)} + 2\beta\ddot{\boldsymbol{D}}^{(n+1)}\right\} \tag{26}$$

$$\dot{\boldsymbol{D}}^{(n+1)} = \dot{\boldsymbol{D}}^{(n)} + \Delta t\left\{(1-\gamma)\ddot{\boldsymbol{D}}^{(n)} + \gamma\ddot{\boldsymbol{D}}^{(n+1)}\right\} \tag{27}$$

where n is the step number and Δt is the integration time step. On the basis of the Taylor expansion of first order of the geometrical relation between the member lengths and the nodal positions, Equation (26) gives the following equation:

$$\boldsymbol{f}(\boldsymbol{D}^{(n+1)}) = \boldsymbol{f}(\boldsymbol{D}^{(n)}) + \boldsymbol{J}\left[\Delta t\dot{\boldsymbol{D}}^{(n)} + \frac{\Delta t^2}{2}\left\{(1-2\beta)\ddot{\boldsymbol{D}}^{(n)} + 2\beta\ddot{\boldsymbol{D}}^{(n+1)}\right\}\right] \tag{28}$$

Substituting Eqs.(27) and (28) into the equation of motion (21) for the $(n+1)$th step, we obtain

$$\begin{aligned}\boldsymbol{M}\ddot{\boldsymbol{D}}^{(n+1)} &+ \boldsymbol{C}\left[\dot{\boldsymbol{D}}^{(n)} + \Delta t\left\{(1-\gamma)\ddot{\boldsymbol{D}}^{(n)} + \gamma\ddot{\boldsymbol{D}}^{(n+1)}\right\}\right] \\ &+\boldsymbol{J}^T\boldsymbol{K}_r\left[\boldsymbol{f}(\boldsymbol{D}^{(n)}) + \boldsymbol{J}\left[\Delta t\dot{\boldsymbol{D}}^{(n)} + \frac{\Delta t^2}{2}\left\{(1-2\beta)\ddot{\boldsymbol{D}}^{(n)} + 2\beta\ddot{\boldsymbol{D}}^{(n+1)}\right\}\right] - \boldsymbol{l}\right] = \boldsymbol{F} - \boldsymbol{J}^T\boldsymbol{q}\end{aligned} \tag{29}$$

Paying attention to $\ddot{\boldsymbol{D}}^{(n+1)}$, this equation is rearranged as

$$\begin{aligned}\left(\boldsymbol{M} + \gamma\Delta t\boldsymbol{C} + \beta\Delta t^2\boldsymbol{J}^T\boldsymbol{K}_r\boldsymbol{J}\right)\ddot{\boldsymbol{D}}^{(n+1)} &= \boldsymbol{F} - \boldsymbol{J}^T\left\{\boldsymbol{q} + \boldsymbol{K}_r\left(\boldsymbol{f}(\boldsymbol{D}^{(n)}) - \boldsymbol{l}\right)\right\} - \left(\boldsymbol{C} + \Delta t\boldsymbol{J}^T\boldsymbol{K}_r\boldsymbol{J}\right)\dot{\boldsymbol{D}}^{(n)} \\ &\quad - \left\{(1-\gamma)\Delta t\boldsymbol{C} + \frac{1-2\beta}{2}\Delta t^2\boldsymbol{J}^T\boldsymbol{K}_r\boldsymbol{J}\right\}\ddot{\boldsymbol{D}}^{(n)}\end{aligned} \tag{30}$$

Using the expression of nodal stiffness matrix Equation (25), the above equation is rewritten as follows:

$$\begin{aligned}\left(\boldsymbol{M} + \gamma\Delta t\boldsymbol{C} + \beta\Delta t^2\boldsymbol{K}\right)\ddot{\boldsymbol{D}}^{(n+1)} &= \boldsymbol{F} - \boldsymbol{J}^T\left\{\boldsymbol{q} + \boldsymbol{K}_r\left(\boldsymbol{f}(\boldsymbol{D}^{(n)}) - \boldsymbol{l}\right)\right\} - \left(\boldsymbol{C} + \Delta t\boldsymbol{K}\right)\dot{\boldsymbol{D}}^{(n)} \\ &\quad - \left\{(1-\gamma)\Delta t\boldsymbol{C} + \frac{1-2\beta}{2}\Delta t^2\boldsymbol{K}\right\}\ddot{\boldsymbol{D}}^{(n)}\end{aligned} \tag{31}$$

This equation can be represented in the following form as

$$\hat{\boldsymbol{M}}\ddot{\boldsymbol{D}}^{(n+1)} = \hat{\boldsymbol{F}} \tag{32}$$

where

$$\hat{\boldsymbol{M}} = \boldsymbol{M} + \gamma\Delta t\boldsymbol{C} + \beta\Delta t^2\boldsymbol{K} \tag{33}$$

$$\hat{\boldsymbol{F}} = \boldsymbol{F} - \boldsymbol{J}^T\left\{\boldsymbol{q} + \boldsymbol{K}_r\left(\boldsymbol{f}(\boldsymbol{D}^{(n)}) - \boldsymbol{l}\right)\right\} - (\boldsymbol{C} + \Delta t\boldsymbol{K})\,\dot{\boldsymbol{D}}^{(n)} - \left\{(1-\gamma)\Delta t\boldsymbol{C} + \frac{1-2\beta}{2}\Delta t^2\boldsymbol{K}\right\}\ddot{\boldsymbol{D}}^{(n)} \tag{34}$$

5.2 Numerical Integration

We consider the typical situation where the truss structural system has several nodes fixed on a basement. The motion of the basement nodes and the external force on the other nodes are assumed to be given.

Nodal positions vector $\boldsymbol{D}$ can be represented as $\boldsymbol{D} = [\boldsymbol{D}_U^T, \boldsymbol{D}_C^T]^T$, where $\boldsymbol{D}_U$ and $\boldsymbol{D}_C$ correspond to the unconfined or free nodal elements and the confined or basement nodal elements, respectively. On the basis of this representation, Equation (32) can be rewritten as

$$\hat{\boldsymbol{M}}_{UU}\ddot{\boldsymbol{D}}_U^{(n+1)} + \hat{\boldsymbol{M}}_{UC}\ddot{\boldsymbol{D}}_C^{(n+1)} = \hat{\boldsymbol{F}}_U \tag{35}$$

$$\hat{\boldsymbol{M}}_{CU}\ddot{\boldsymbol{D}}_U^{(n+1)} + \hat{\boldsymbol{M}}_{CC}\ddot{\boldsymbol{D}}_C^{(n+1)} = \hat{\boldsymbol{F}}_C \tag{36}$$

where the subscripts U and C represent the parts of elements corresponding to $\boldsymbol{D}_U$ and $\boldsymbol{D}_C$, respectively. Since the external nodal force $\boldsymbol{F}_U(t)$ is assumed to be given, $\hat{\boldsymbol{F}}_U$ is calculated in terms of the corresponding part of Equation (34). The motion of the basement nodes $\boldsymbol{D}_C(t)$ is also assumed to be given. Hence, Equation (35) is solved for $\ddot{\boldsymbol{D}}_U^{(n+1)}$ as

$$\ddot{\boldsymbol{D}}_U^{(n+1)} = \hat{\boldsymbol{M}}_{UU}^{-1}\left(\hat{\boldsymbol{F}}_U - \hat{\boldsymbol{M}}_{UC}\ddot{\boldsymbol{D}}_C^{(n+1)}\right) \tag{37}$$

On the basis of the obtained nodal acceleration at the $(n+1)$th step, $\ddot{\boldsymbol{D}}^{(n+1)} = [(\ddot{\boldsymbol{D}}_U^{(n+1)})^T, (\ddot{\boldsymbol{D}}_C^{(n+1)})^T]^T$, the nodal position and velocity vectors at the $(n+1)$th step are calculated with Eqs.(26) and (27). The force on the basement nodes $\boldsymbol{F}_C$ can be obtained based on Equation (34), in terms of $\hat{\boldsymbol{F}}_C$ calculated with Equation (36).

5.3 Procedure for Numerical Simulation

Since we deal with adaptive truss structures having geometrical and mechanical adaptability in this study, all of the matrices and vectors are not constant in general. In particular, the elements of member stiffness $\boldsymbol{K}_r$ can change drastically in the case of wire members and can depend on the deformation progressing directions in the case of SMA members. The following procedure is developed in order to cope with this situation:

[0] Set an adequate value to time step Δt. The step number is $n = 0$. Reference lengths $\boldsymbol{l}$ is determined so that $\boldsymbol{r} = 0$.

[1] Update matrices $\boldsymbol{M}$, $\boldsymbol{C}_h$, $\boldsymbol{K}_r$ and $\boldsymbol{J}$ and vector $\boldsymbol{q}$. It should be noted that member stiffness $\boldsymbol{K}_r$ can be affected by the direction of deformation progression as expressed in Equation (13).

[2] Calculate the nodal damping and stiffness matrices, $\boldsymbol{C}$ and $\boldsymbol{K}$, in terms of Eqs.(22) and (25).

[3] Calculate $\hat{\boldsymbol{M}}$ and $\hat{\boldsymbol{F}}$ in terms of Eqs.(33) and (34). Calculate Equation (37) and obtain nodal acceleration $\ddot{\boldsymbol{D}}^{(n+1)}$, nodal velocity $\dot{\boldsymbol{D}}^{(n+1)}$ in terms of Equation (27), and nodal positions $\boldsymbol{D}^{(n+1)}$ in terms of Equation (26).

[4] Calculate Equation (23) as $\boldsymbol{r} = \boldsymbol{f}(\boldsymbol{D}^{(n+1)}) - \boldsymbol{l}$. Evaluate the signs of elements of $\boldsymbol{r}$ corresponding to SMA members, that is the deformation progressing direction to be referred in **[1]**.

[5] Update the reference lengths as $\boldsymbol{l} \leftarrow \boldsymbol{l} + \boldsymbol{r}$ and reset the obtained deformation $\boldsymbol{r} \leftarrow 0$. Update the state of SMA members and the relevant variables in accordance with the deformation.

[6] Set $n \leftarrow n + 1$ and continue from **[1]** until the end of simulation process.

The successive modification of reference length $\boldsymbol{l}$ is adopted in order to deal with the nonlinearity of the system. In the above procedure, $\boldsymbol{r}$ obtained in **[4]** denotes the member deformation progression within a single time step. The time step Δt applied for the numerical simulation process should be significantly small compared to the case of the ordinary truss structure, in order to reduce the discretization error due to the drastic change in stiffness of wire and SMA members.

6. Example Dynamic Simulation Results

In order to demonstrate the feasibility of the proposed dynamics calculation of adaptive truss, we conduct two types of simulations: dynamic behaviors of geometry adaptation motion and dynamic responses to basement motion.

6.1 Initial Static Equilibrium Condition

In the current simulation studies, the truss systems to be simulated are assumed to be in static equilibrium condition at the initial point. We have to calculate this static equilibrium condition prior to the dynamic simulation calculation, in such a case that an external nodal force or non-zero axial forces of truss members have to be taken into consideration at the initial state. In order to determine the initial condition of dynamic simulation, we conduct the following kinematic simulation assuming quasi-static motion.

Ignoring the dynamic terms in Equation (20), we obtain the following static equilibrium equation:

$$\boldsymbol{J}^T \boldsymbol{K}_r \boldsymbol{r} = \boldsymbol{F} - \boldsymbol{J}^T \boldsymbol{q} \tag{38}$$

Owing to the quasi-static assumption, the deformation $\boldsymbol{r}$ is assumed to be small enough; on the basis of the linear relation $\boldsymbol{r} = \boldsymbol{J}\boldsymbol{U}$ with the nodal displacement $\boldsymbol{U}$, we obtain

$$\boldsymbol{K}\boldsymbol{U} = \boldsymbol{F} - \boldsymbol{J}^T \boldsymbol{q} \tag{39}$$

where the nodal stiffness $\boldsymbol{K}$ is given as Equation (25). In order to calculate the static equilibrium condition corresponding to the assumed situation, the following process is iteratively performed in a quasi-static manner from an appropriate equilibrium state:

- Solve Equation (39) for $\boldsymbol{U}$ under the constraint of fixed basement nodes.
- Calculate $\boldsymbol{r} = \boldsymbol{J}\boldsymbol{U}$.
- Update $\boldsymbol{l} \leftarrow \boldsymbol{l} + \boldsymbol{r}$ and $\boldsymbol{D} \leftarrow \boldsymbol{D} + \boldsymbol{U}$.
- Update $\boldsymbol{J}$, $\boldsymbol{K}_r$, $\boldsymbol{K}$, $\boldsymbol{F}$, $\boldsymbol{\rho}$ and $\boldsymbol{q}$ accordingly.

6.2 Geometry Adaptation Motion

An adaptive truss has geometry adaptation capability in the case that it has a number of length-adjustable truss members. Figure 3 shows such examples of geometry adaptation motion. Figure 3(a) shows an example motion of a conventional VGT having a statically determinate topology and rigid telescopic-type actuators. In the case that the length-adjustable members are wires to be wound and unwound for actuation, an adaptive truss has to have a statically indeterminate topology as shown in Figure 3(b), since the wires cannot take any compressive force.

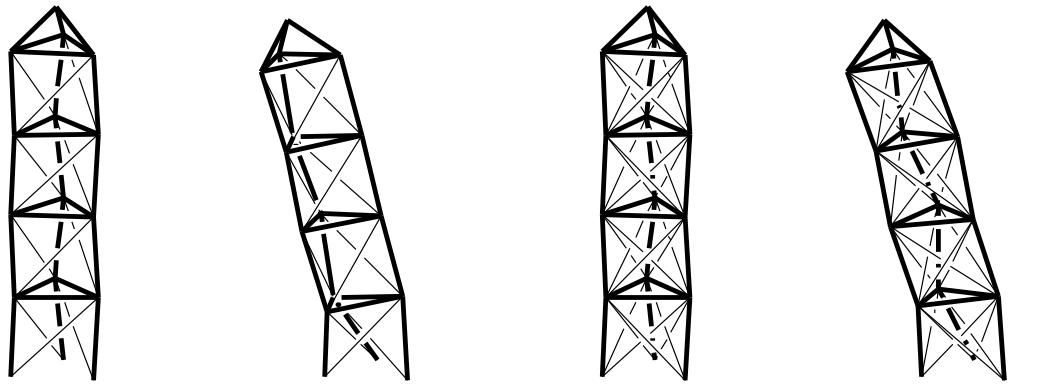

(a1) Initial posture $\boldsymbol{x}_N = [0.0, 0.0, 4.5]$(m) (a2) Final posture $\boldsymbol{x}_N = [-1.0, 0.0, 4.3]$(m) (b1) Initial posture $\boldsymbol{x}_N = [0.0, 0.0, 4.5]$(m) (b2) Final posture $\boldsymbol{x}_N = [-1.0, 0.0, 4.3]$(m)

(a) With rigid actuators (statically determinate configuration) (b) With wire actuators (statically indeterminate configuration)

Figure 3. Example geometry adaptation motion: configurations and postures

In this simulation study, the geometry adaptation motion is determined in an incremental manner. We denote the member lengths increment as $\Delta \boldsymbol{l} = [\Delta \boldsymbol{l}_A^T, \Delta \boldsymbol{l}_F^T]^T$, where $\Delta \boldsymbol{l}_A$ corresponds to the actuated members and $\Delta \boldsymbol{l}_F = 0$ corresponds to the fixed-length non-actuated members. The actuating increment $\Delta \boldsymbol{l}_A$ is determined based on the specified increment $\Delta \underline{\boldsymbol{x}}_N$ of the nodal position at the peripheral end, as the solution of the following minimization problem:

$$\text{Minimize} \quad g = g(\Delta \boldsymbol{X}) \quad \text{with respect to} \quad \Delta \boldsymbol{X} \quad \text{subject to} \begin{cases} \dfrac{\partial \boldsymbol{l}_F}{\partial \boldsymbol{X}} \Delta \boldsymbol{X} = \boldsymbol{B}_F \dfrac{\partial \boldsymbol{l}}{\partial \boldsymbol{X}} \Delta \boldsymbol{X} = 0 \\ \Delta \boldsymbol{X}_C = \boldsymbol{B}_C \Delta \boldsymbol{X} = 0 \\ \Delta \boldsymbol{x}_N = \boldsymbol{B}_N \Delta \boldsymbol{X} = \Delta \underline{\boldsymbol{x}}_N \end{cases} \tag{40}$$

where the constraints are the constant lengths of non-actuated members and the fixed position of the basement nodes, in addition to the specified increment of the nodal position at the peripheral end. The Jacobian matrix $\partial \boldsymbol{l} / \partial \boldsymbol{X}$ is given in section 2.2 and $\boldsymbol{B}_F$, $\boldsymbol{B}_B$ and $\boldsymbol{B}_N$ are the boolean matrices corresponding to the constraints. In the current study, the introduced objective function g intends to suppress the magnitude of increment of actuation motion and is expressed as

$$g(\Delta \boldsymbol{X}) = \frac{1}{2} (\Delta \boldsymbol{l}_A)^T \Delta \boldsymbol{l}_A = \frac{1}{2} \left(\boldsymbol{B}_A \frac{\partial \boldsymbol{l}}{\partial \boldsymbol{X}} \Delta \boldsymbol{X} \right)^T \boldsymbol{B}_A \frac{\partial \boldsymbol{l}}{\partial \boldsymbol{X}} \Delta \boldsymbol{X} = \Delta \boldsymbol{X}^T \left[\left(\frac{\partial \boldsymbol{l}}{\partial \boldsymbol{X}} \right)^T \boldsymbol{B}_A^T \boldsymbol{B}_A \frac{\partial \boldsymbol{l}}{\partial \boldsymbol{X}} \right] \Delta \boldsymbol{X} \tag{41}$$

where $\boldsymbol{B}_A$ is the corresponding boolean matrix. Problem (40) can be solved by means of a generalized inverse (Rao & Mitra, 1971) of the Jacobian matrix.

The specification of the adaptive trusses adopted in this simulation is assumed to be as follows:

- The material of the truss members is aluminum.
- The cross-section of the non-actuated truss members is 50mm^2.
- The cross-section of the length-adjustable members is 1mm^2. This is common to both rigid telescopic members and wire members.
- A mass of 10kg is attached to the peripheral end node.

It should be noted that a rigid telescopic length-adjustable actuator of 1mm^2 cross-section is unrealistic; however, it is adopted in this simulation study in order to compare the dynamic behaviors of adaptive trusses that consisting only of rigid members and that having wire members which cannot take any compressive force.

Figures 3(a1) and 3(b1) are the initial postures corresponding to the position of the peripheral end node $\boldsymbol{x}_N = [0.0, 0.0, 4.5]^T$(m). The intermediate nodal positions at the height of 1m and 3m are twisted 10 degrees in order

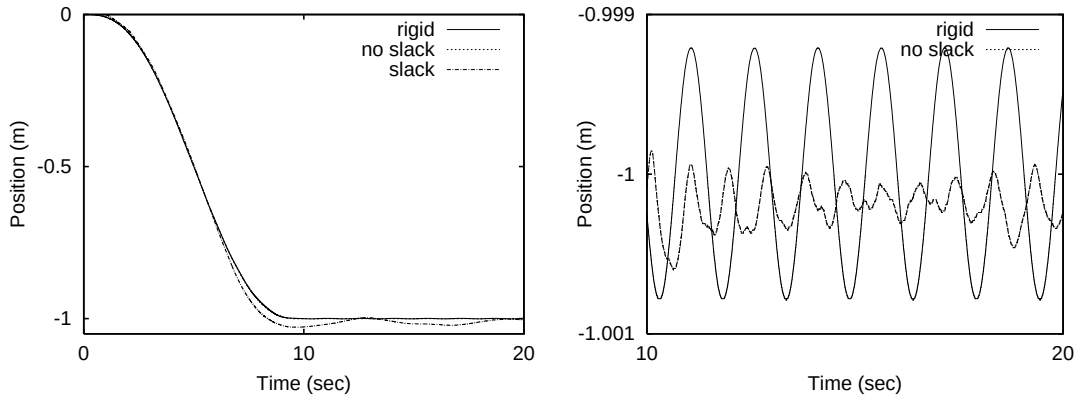

(a) Horizontal motion of peripheral end (b) Magnified residual vibration

Figure 4. Dynamic behavior of peripheral end node based on geometry adaptation motion

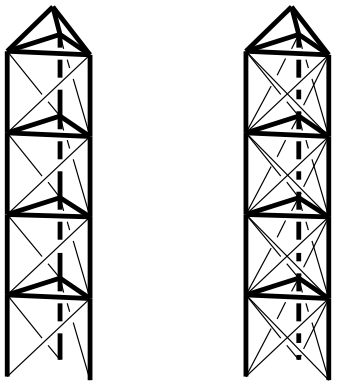

(a) Spring-dashpot (b) SMA-wire

Figure 5. Adaptive trusses for basement vibration simulations

to avoid the singularity of the Jacobian matrix for the geometry adaptation motion. Figures 3(a2) and 3(b2) are the final postures corresponding the target position of the peripheral end node $\underline{\boldsymbol{x}}_N = [-1.0, 0.0, 4.3]^T$(m), that is, displaced 1m leftward and 0.2m downward, respectively. The two postures are different due to the difference in the kinematic condition such as the topology.

Figure 4 shows the simulated dynamic behaviors of the peripheral end nodes in horizontal direction, corresponding to the motion of the adaptive trusses attaining the final postures shown in Figures 3(a2) and 3(b2) from the initial postures shown in Figures 3(a1) and 3(b1) in 10s. The time step Δt of numerical integration is 10μs. This extremely short time step is adopted to deal with the drastic change in stiffness of the wire members. In these graphs, 'rigid' indicates the behavior of the adaptive truss consisting of rigid telescopic actuators and 'no slack' and 'slack' indicate those of the adaptive truss with wire actuators, where 'slack' signifies that the wires are loosened 1mm from the lengths determined by the motion planning. On the basis of the result shown in Figure 4(a), the influence of the loosening is significant. The magnified residual vibration shown in Figure 4(b) demonstrates that the vibration is apparently sinusoidal for 'rigid' but is clearly different for 'no slack'. This difference indicates a significant influence of the the mechanical characteristics of wires of zero compressive stiffness, even in the case of no slack condition.

6.3 Basement Motion

An adaptive truss can have various dynamic capabilities by installing different types of truss members. We conduct dynamic simulations in order to examine dynamic responses of such adaptive trusses to basement motions. Figure 5 shows the configurations of adaptive trusses adopted in the simulations. Figure 5(a) is a statically determinate adaptive truss having spring-dashpot mechanisms as its diagonal truss members. Figure 5(b) is a statically indeterminate adaptive truss. This adaptive truss is assumed to have ordinary wires or SMA wires as its diagonal truss members. The specification of the adaptive trusses adopted in this simulation is given as follows referring to the specification in the previous simulations:

- The material of the vertical and horizontal truss members is alminum. The cross-section of these truss members is 50mm^2.
- A mass of 10kg is attached to the peripheral end node.
- As the ordinary wire members, alminum wires of 1mm^2 cross-section are adopted.
- For the spring-dashpot members, a stiffness coefficient of 70kN/m and a damping coefficient of 50Ns/m are adopted.
- The SMA wires are assumed to be of NiTi alloy having the piecewise linear characteristics shown in Figure 2(b) and of 1mm^2 cross-section. All these SMA wires are in austenite phase in this study; that is, they exhibit pseudo-elasticity. Two type of values are adopted for the initial strain: 0% and 3%.

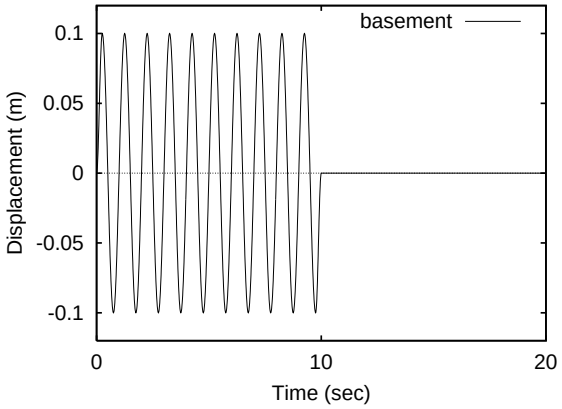

(a) Oscillatory motion

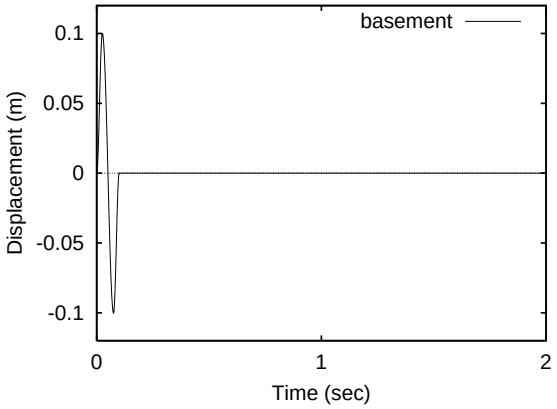

(b) Single-shot motion

Figure 6. Assumed basement motions

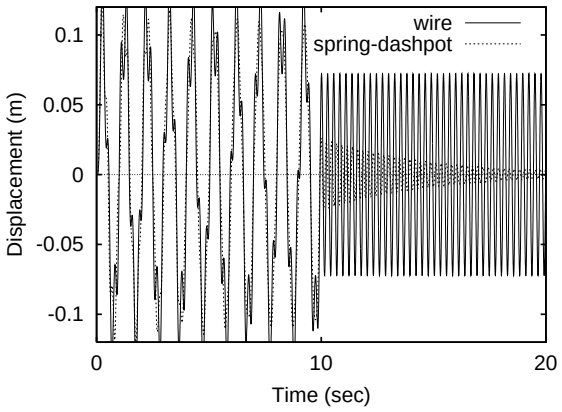

(a) Wire and spring-dashpot member

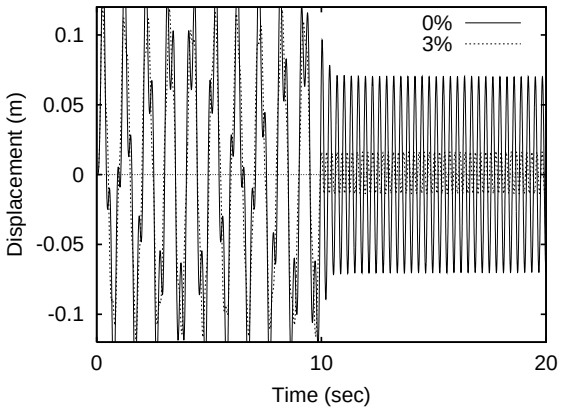

(b) SMA wire member

Figure 7. Response to oscillatory basement motion shown in Figure 6(a)

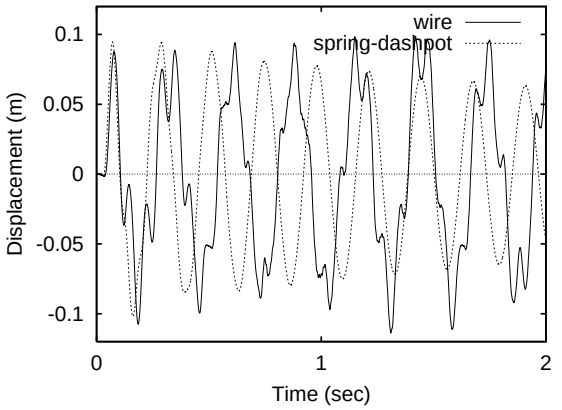

(a) Wire and spring-dashpot member

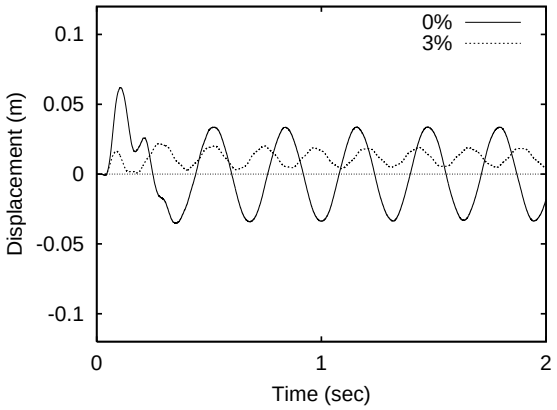

(b) SMA wire member

Figure 8. Response to single-shot basement motion shown in Figure 6(b)

The two basement motions adopted in the simulations are shown in Figure 6. The oscillatory motion shown in Figure 6(a) is of 1Hz frequency, 0.1m magnitude and 10s duration. The single-shot motion shown in Figure 6(b) is of 0.1m magnitude and 0.1s duration. Figures 7 and 8 show the resultant responses of adaptive trusses in terms of the simulated horizontal motions of the peripheral end node. Figures 7 and 8 respectively correspond to the oscillatory basement motion shown in Figure 6(a) and the single-shot basement motion shown in Figure 6(b).

As shown in Figure 7(a), an attenuation of residual vibration is demonstrated in the case of the adaptive truss having spring-dashpot members. On the basis of the adaptive truss having SMA wires, we have obtained significantly different responses between the cases of initial strain values 0% and 3% of SMA wires as shown in Figure 7(b). In the case of 0% initial strain, the truss cannot take advantage of the hysteretic characteristic of the SMA members, since the stress and strain of the SMA wires are basically in the proportional linear part of the assumed piecewise linear characteristics of SMA shown in Figure 2(b). In the case of 3% initial strain of SMA wires, it is demonstrated that the residual vibration is rapidly reduced to less than a third. In contrast to the case of spring-dashpot members, however, the reduction of the residual vibration remains at a certain level in this case. This is because the piecewise linear model shown in Figure 2(b) does not take into account the minor hysteresis loop of the actual shape memory alloy.

In the case of the single-shot basement motion shown in Figure 6(b), we can see a conspicuous difference between the responses of the cases of ordinary wires and spring-dashpot members shown in Figure 8(a), and the responses of the case of SMA wire members shown in Figure 8(b). The responses shown in Figure 8(a) demonstrate the decrease of vibration by means of the spring-dashpot members in 2s. The magnitude of vibration shown in Figure 8(b) is significantly smaller than the case shown in Figure 8(a). This is mostly due to the relatively flat or low-stiffness part of the stress-strain relation of the SMA characteristics shown in Figure 2(b). This effect of vibration alleviation can also be confirmed based on the comparison of the two cases shown in Figure 8(b); the adaptive truss of SMA wires with 3% initial strain takes more advantage of this SMA characteristic.

7. Concluding Remarks

An adaptive truss structure system is expected to be able to perform various functions in accordance with the types of truss members installed. In the current study, we have dealt with the dynamic simulation of adaptive truss consisting of truss members of different mechanical properties.

Models of mechanical behaviors of ordinary rigid member, spring-dashpot member and SMA member were considered; they can also be of wire that cannot take any compressive axial force. A model in general form is given; other types of truss members can be dealt with based on the formulation. The geometrical relation and the equation of motion of adaptive truss have been formulated in general form. A dynamic simulation method that can take into account the basement vibration was developed based on the Newmark β numerical integration approach.

Feasibility of the proposed dynamic simulation approach has been demonstrated with a number of calculation examples. The obtained results show the characteristic behaviors of the adopted functional truss members. It has been also shown that the adaptive truss having SMA wire members is expected to have some promising dynamic capabilities, although the current characteristic model of SMA is simply piecewise linear.

On the basis of the developed dynamic simulation, we can now design an adaptive truss having some intended dynamic characteristics that consists of various types of functional truss members. This is possibly our future work.

References

Chen, G.-S., & Wada, B. K. (1993). Adaptive Truss Manipulator Space Crane Concept. *Journal of Spacecraft and Rockets, 30*(1), 111–115. http://dx.doi.org/10.2514/3.25477

Dos Santos, F. A., Rodrigues, A., & Micheletti, A. (2015). Design and Experimental Testing of an Adaptive Shape-Morphing Tensegrity Structure, with Frequency Self-Tuning Capabilities, Using Shape-Memory Alloys. *Smart Materials and Structures, 24*(10), Paper 105008. http://dx.doi.org/10.1088/0964-1726/24/10/105008

Dunlop, R., & Garcia, A. C. (2002). A Nitinol Wire Actuated Stewart Platform, *Proceedings of 2002 Australasian Conference on Robotics and Automation*, 122–127.

Dutta, S. M., & Ghorbel, F. H. (2005). Differential Hysteresis Modeling of a Shape Memory Alloy Wire Actuator. *IEEE Transaction on Mechatronics, 10*(2), 189–197. http://dx.doi.org/10.1109/TMECH.2005.844709

Hanahara, K., & Tada, Y. (2000). Design of Statically Indeterminate Geometry Adaptive Truss with Wire Member

Actuators. *Eleventh International Conference on Adaptive Structures and Technologies*, 227–234, Technomic.

Hanahara, K., & Tada, Y. (2002). Motion of Variable Geometry Truss for Momentum Management in Spacecraft. *AIAA Journal, 40*(8), 1673–1676. http://dx.doi.org/10.2514/2.1839

Hanahara K., & Tada, Y. (2004). Variable Geometry Truss Actuated by Wire Members (Basic Consideration on Practical Actuation Mechanism). *15th International Conference on Adaptive Structures and Technologies*.

Hanahara, K., Kakihara, K., Tada, Y., & Usami, Y. (2006). A Prototype of Wire-Actuated Variable Geometry Truss (Design and Kinematics of 2D Experimental System), *Proceedings of ICAST2006: 17th International Conference on Adaptive Structures and Technologies*, 187–194.

Hanahara, K., & Tada, Y. (2008). Variable Geometry Truss with SMA Wire Actuators (Basic Consideration on Kinematical and Mechanical Characteristics). *Proceedings of the 19th International Conference on Adaptive Structures and Technologies*.

Hanahara, K., & Tada, Y. (2014). Adaptive Structural Shape Refinement by Means of SMA Wire (Verification of Basic Idea via Simulation Studies). *International Conference on Adaptive Structures and Technologies*.

Hughes, P. C., Sincarsin, W. G., & Carroll, K. A. (1991). Trussarm – A Variable-Geometry-Truss Manipulator. *Journal of Intelligent Material Systems and Structures, 2*(2), 148–160. http://dx.doi.org/10.1177/1045389X9100200202

Lagoudas, D. C. eds. (2008). *Shape Memory Alloys (Modeling and Engineering Applications)*, Springer.

Merlet, J.-P. (2006). *Parallel Robots, 2nd ed.* Springer.

Miura, K., Furuya, H., & Suzuki, K. (1985). Variable Geometry Truss and Its Application to Deployable Truss and Space Crane Arm. *Acta Astronautica, 12*(7/8), 599–607. http://dx.doi.org/10.1016/0094-5765(85)90131-6

Newmark, N. M. (1959). A Method of Computation for Structural Dynamics. *ASCE Journal of the Engineering Mechanics Division*, 85(EM3), 67–94.

Ramesh, A. V., Utku, S., Wada, B. K., & Chen, G. S. (1990). Effect of Imperfections on Static Control of Adaptive Structure as a Space Crane. *Journal of Intelligent Material Systems and Structures, 1*(3), 309–326. http://dx.doi.org/10.1177/1045389X9000100304

Rao, C. R., & Mitra, S. K. (1971). *Generalized Inverse of Matrices and its Applications*, Chap. 3, John Wiley & Sons.

Seguchi, Y., Tanaka, M., Yamaguchi, T., Sasabe, Y., & Tsuji, H. (1990). Dynamic Analysis of a Truss-Type Flexible Robot Arm *JSME International Journal Series III, 33*(2), 183–190. http://dx.doi.org/10.1299/jsmec1988.33.183

Senda, K., Ando, A., & Murotsu, Y. (1995). Optimal Posture of a Redundant VGT for Docking, *Sixth International Conference on Adaptive Structures*, 439–449, Technomic.

Stewart, D. (1965-66). A platform with six degrees of freedom. *Proceedings of Institution of Mechanical Engineers, 180*(15), Part 1, 371–386.

Tanaka, M., Seguchi, Y., & Hanahara, K. (1991). Kinematics of Adaptive Truss Permitting Nodal Offset (Configuration and Workspace Reach). *Journal of Intelligent Material Systems and Structures, 2*(3), 301–327. http://dx.doi.org/10.1177/1045389X9100200304

Wada, B. K., Fason, J. L., & Crawley, E. F. (1990). Adaptive Structures. *Journal of Intelligent Material Systems and Structures, 1*(2), 157–174. http://dx.doi.org/10.1177/1045389X9000100202

Yang, F., Sedaghati, R., Younesian, D., & Esmailzadeh, E. (2005). Optimal Placement of Active Bars in Smart Structures. *Proceedings of the IEEE International Conference on Mechatronics & Automation*. http://dx.doi.org/10.1109/ICMA.2005.1626513